Cosmic-ray physics and the Pierre Auger Observatory

M.T. Dova
IFLP (Conicet-UNLP), National University of La Plata, La Plata, Argentina and Pierre Auger Observatory, Malargüe, Argentina

Abstract
One of the foremost issues in astrophysics today is that of the origin of ultra-high-energy cosmic rays. The Pierre Auger Observatory is a broadly based international effort to make a high-statistics study of the upper-end of the cosmic-ray spectrum. Auger is the first experiment designed to work in a hybrid detection mode. It consists of an array of 1600 particle detectors spread over 3000 km^2 and four fluorescence telescopes placed on the boundaries of the surface array. Recent measurements from Auger of the energy spectrum and mass composition above 10^{18} eV are described.

1 Introduction

Some 40 years after the discovery of ultra-high-energy cosmic rays [1], fundamental questions regarding their origin and nature lack definitive answers. The highest primary energy measured thus far is $E \sim 10^{20.5}$ eV [2], corresponding to a nucleon–nucleon centre-of-mass energy $\sqrt{s} \sim 10^{5.9}$ GeV/$\sqrt{A}$, where A is the mass number of the primary particle. The existence of these particles, the most energetic known in the Universe, challenges our current understanding of physics. From the perspective of astrophysics, one must identify where and how in the Universe these particles obtain such high energies. A failure to uncover such mechanisms may lead one to postulate new physics to explain the phenomenon. From the perspective of particle physics, ultra-high-energy cosmic-ray interactions are orders of magnitude beyond what can be achieved in current (and future) terrestrial collider experiments and may open a window to energy and kinematic regions previously unexplored in the study of fundamental interactions. From both perspectives, the tantalizing possibility of new physics that may be found in the study of ultra-high-energy cosmic rays continues to motivate current and future cosmic-ray experiments [3].

2 About the origin of high-energy cosmic-ray particles

The conventional theory of cosmic rays posits that Supernova remnants (SNRs) are the site of acceleration of cosmic rays below 10^{15} eV. However, it is often argued that the known acceleration mechanisms have problems in acquiring energies in excess of 10^{15} eV at SNRs. The acceleration is assumed to take place at the shock front associated with the supersonic motions of the expanding shell, and the particles are energized through diffuse acceleration *à la Fermi*. The magnetic scattering provided by the interstellar medium (ISM) is insufficient to warrant the acceleration of cosmic rays beyond that energy. It was then proposed in Ref. [4] that a self-generated amplified magnetic field in the vicinity of the source can exceed the ambient field, i.e., the accelerated particles generate a large magnetic field.

It is believed that at some energy of the order of 10^{18} eV all observed cosmic rays (CRs) come from extragalactic sources, because they cannot be contained in the Galaxy long enough to be accelerated to such energies. Where exactly the transition from galactic to extragalactic origin happens is an open question that should be answered with the study of the ultra-high-energy cosmic ray (UHECR) region of the spectrum.

A complete discussion of most of the models for the production of UHECRs can be found in the reviews [5, 6] and references therein. Production mechanisms have been commonly classified into two groups: a) bottom-up models, which consider conventional acceleration of UHECRs in rapidly evolving processes in known astrophysical objects [7–9] and b) top-down models suggesting that particles are

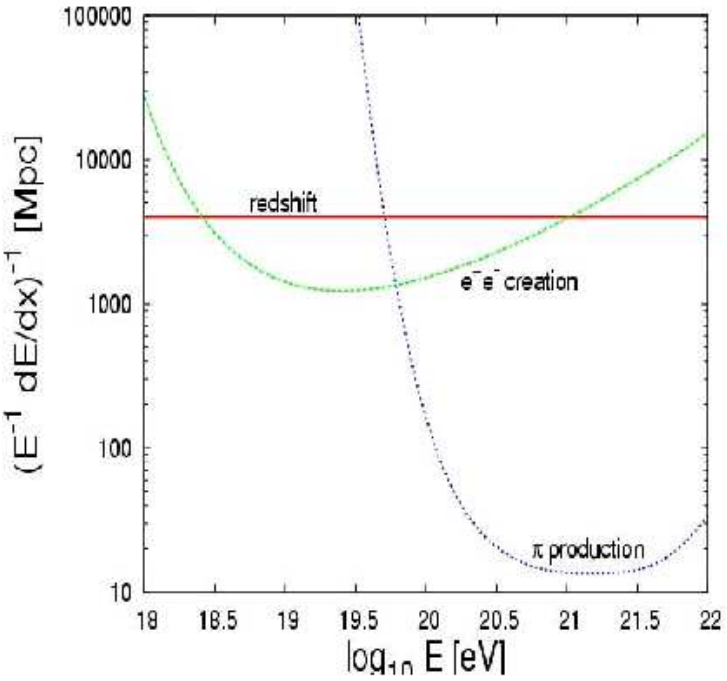

Fig. 1: Proton energy losses in the CMB field

not accelerated but rather that they are stable decay products of supermassive particles [5]. The source of these exotic particles could be topological defect (TD) relics from early Universe phase transitions associated with spontaneous symmetry breaking underlying unified models of high-energy interactions. A general characteristic of top-down models is that, alongside protons, many photons and neutrinos are also produced giving an extra signature to these processes. Detection of neutrinos would be an important clue to identification of the UHECR sources.

2.1 Propagation

A key issue to be considered in the search for the origin of extremely high energy cosmic rays is the opacity of the cosmic microwave background radiation (CMB) to the propagation of UHECRs which yields the well-known effect called the Greisen–Zatsepin–Kuzmin (GZK) cut-off. The first treatments [10] indicated a sharp cut-off for cosmic rays with energies above 5×10^{19} eV due to the photopion production process $\gamma + p \rightarrow \Delta \rightarrow p/n\pi$. In Fig. 1 we see the proton energy losses in the CMB field distinguishing the three different channels: pair production, photopion production, and adiabatic energy losses due to redshift. A similar phenomenon of energy degradation occurs for nuclei due to the process of photodisintegration which is very important in the region of giant resonances, but here the diffuse infrared background is of greater importance than the 2.7 K radiation. Many calculations have been performed using various techniques to study the modification of the cosmic-ray spectrum [11] and the general features are now well established. Using the calculated energy losses it is straightforward to obtain the energy degradation of UHECRs in terms of the flight distance. The interaction of protons with photons of the CMB then constrains the proximity of the UHECR sources to Earth and the effect is seen as a cut-off in the spectrum. Above 100 Mpc the observed energy is below 10^{20} eV regardless of the initial value.

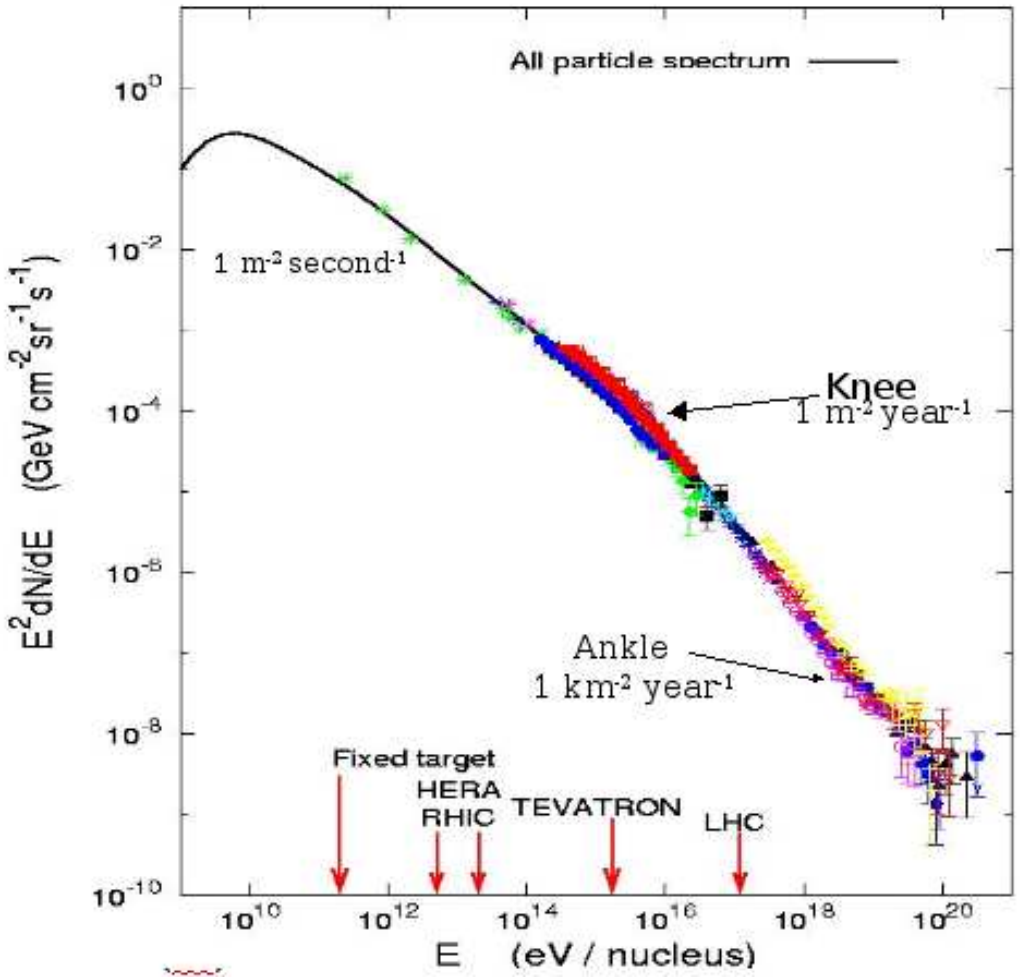

Fig. 2: Differential energy spectrum of primary cosmic rays over a broad energy range

3 Spectrum, arrival directions and composition of UHECRs in the pre-Auger era

Figure 2 shows the particle spectrum (without distinction of charge and mass) as measured by many different experiments using different techniques. For primary energy $E > 1$ GeV the observed cosmic-ray flux can be described by a series of power laws with the flux falling about three orders of magnitude for each decade increase in energy. In the decade centred at $\sqrt{s}|_{\rm knee} \sim 10^{3.4}$ GeV$/\sqrt{A}$, the spectrum steepens from $E^{-2.7}$ to $E^{-3.0}$, forming the feature commonly known as 'the knee'. The spectrum steepens further to $E^{-3.3}$ above $\sqrt{s}|_{\rm dip} \sim 10^{4.5}$ GeV$/\sqrt{A}$, and then flattens to $E^{-2.7}$ at $\sqrt{s}|_{\rm ankle} \sim 10^{5.1}$ GeV$/\sqrt{A}$, forming a feature known as 'the ankle' [12]. Within the statistical uncertainty of existing data, which is large for $E > 10^{20}$ eV, the tail of the spectrum is consistent with a simple extrapolation at that slope to the highest energies. Thus far, for Earth-based accelerators, the record holder for collisions with the highest energy per nucleon is the Tevatron, which countercirculates protons and antiprotons with $\sqrt{s} \simeq 1.8$ TeV. This centre-of-mass energy corresponds closely to that at the knee. The Large Hadron Collider (LHC), now under construction at CERN, will collide protons with protons at $\sqrt{s} \simeq 14$ TeV. This impressive energy is still about a factor of 50 smaller than the centre-of-mass energy of the highest energy cosmic ray so far observed, assuming $A = 1$.

Above 10^{15} eV all the measurements are indirect. If the primary particle is a nucleon or nucleus, the cascade begins with a hadronic interaction and the number of hadrons increases through subsequent interactions. In each generation 30% of the energy is transferred to an electromagnetic cascade by the

rapid decay of the π^0's. Finally, the electromagnetic cascade dissipates $\approx 90\%$ of the primary energy through ionization. The evolution of the extensive air shower (EAS) is then dominated by electromagnetic processes, the growth is governed by bremsstralung and pair production until the energy of the particles fall below the critical energy (at the position of shower maximum, $X_{\max}$) and ionization losses take over from bremsstralung and pair production. Then, the number of electrons and photons begins to decrease, while the number of muons remains more or less the same. There are two main techniques to study UHECRs, a ground array of detectors spread over a large area sampling the particles at given observing levels (surface detectors, SDs), and large-aperture telescopes (fluorescence detectors, FDs). This last technique can be used because during the development of the extensive air showers, the charged secondaries excite the nitrogen molecules with a subsequent emission of fluorescence light.

It is worth mentioning that the energy calibration for ground array experiments is performed using simulation results and hence relies on the assumption of the high-energy hadronic interaction model, nevertheless it is a very robust technique, with 100% duty cycle and a well defined and large aperture. Very succesful SD experiments were Volcano Ranch, Haverah Park, SUGAR, Yakutsk and AGASA. The AGASA array in Japan [13], comprised 111 scintillation detectors each of 2.2 m^2 on a grid of about 1 km spacing. The detectors were connected and controlled through a sophisticated optical fibre network. The AGASA array was closed down in January 2004.

The HiRes experiment in Utah [14], uses the FD technique which provides the most effective way to measure the energy of the primary particles. The nitrogen emits fluorescence radiation isotropically, predominantly in the 300–400 nm band, and this can be observed at distances of ≈ 20 km with arrays of photomultipliers on dark, clear nights. The magnitudes of the signals in the tubes are used to estimate the number of particles along the track of the shower. The primary energy is derived by integrating the longitudinal development curve and multiplying the result by the appropriate $-dE/dx$. This gives a calorimetric estimate of the total energy deposited in the atmosphere. The estimation of the aperture is difficult as it grows with energy. Also a good knowledge of atmospheric properties is crucial for the energy determination. The largest systematics is due to uncertainties in the fluorescence yield efficiency: the number of photons emitted by the shower as it passes through the atmosphere.

An important ingredient in the search for the origin of UHECRs is to locate their sources. It is possible to do particle astronomy selecting those events with the largest magnetic rigidity and check if they can be combined into clusters indicating the direction of a possible source in our vicinity, in particular correlated with distribution of astrophysical objects. In our neighborhood there are two main structures showing an accumulation of objects: the galactic plane on a small scale and the supergalactic plane on a large scale. The latter consists of a structure roughly normal to the galactic plane extending to distance of about 100 Mpc, correlated with a denser distribution of radiogalaxies. Of course, for such analyses it is very important to take into account the effect of the galactic and extragalatic magnetic fields. For example, the trajectories of a proton of 10^{18} eV are very curly for galactic fields of a few μpc and one has to describe the propagation in terms of diffusion and drift. But for a proton at 10^{19} eV the trajectories are straighter. All theses effects are important if UHECRs are due to a few powerful sources, so, many interesting effects could be studied.

To get information about the origin of cosmic rays, studies of anisotropy together with the analysis of the spectrum and composition are mandatory. The present experimental data seem to be consistent with an isotropic distribution of sources, in sharp contrast to the anisotropic distribution of light in the local supercluster. However, there may be clusters. The AGASA experiment has presented an analysis of their extremely high-energy events, suggesting indications of clustering on an angular scale of 2.5° with a probability of chance coincidence of less than 1%. It is remarkable that none of those clusters is on the galactic plane suggesting that UHECRs are most likely extragalactic in origin.

Another ingredient to consider in the search for the origin of these very energetic particles is the chemical composition of the UHECRs detected. In present experiments the interpretation of data, in all cases, depends on the physics of the cascade included in the event generators. Methods of determining the

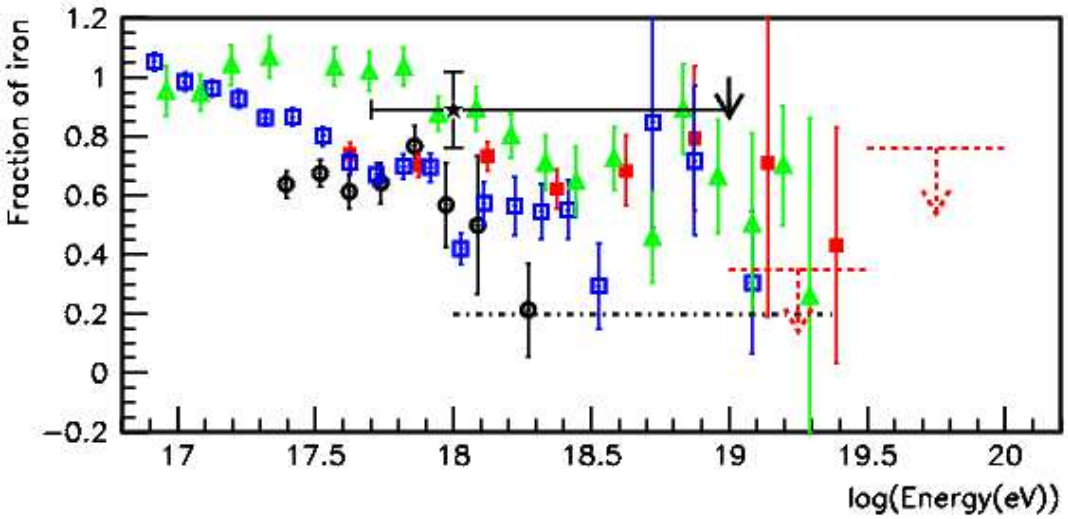

Fig. 3: Fe fraction from various experiments: Fly's Eye (△), AGASA A100 (■), AGASA A1 (□) using SIBYLL 1.6 [([19] and references therein) and Haverah Park [20], using QGSJET98 (○)]. Mean composition determined in Ref. [21] with the corresponding error for the Volcano Ranch energy range using QGSJET98 (★) is shown. The solid line arrow represents a recent result from risetime measurements from Haverah Park [22]. The dashed arrow lines represents upper limits obtained by AGASA presented in Ref. [23]. The dot–dashed horizontal line corresponds to the HiRes results [24].

composition of the primary can be classified into three groups: (i) measurements of $X_{\rm max}$ and fluctuations in the distribution of $X_{\rm max}$ from air–Cerenkov light or fluorescence light emissions, (ii) muon densities, and (iii) measurements that are essentially geometrically based, such as slope of the lateral distribution function (LDF) or the thickness of the shower-front or the shower-front curvature. For a review and discussions see, for example, Ref. [15]. There are hints about photon fluxes above 10^{19} eV but not much is known about hadronic masses, as is evident from Fig. 3 where a summary of the results in the pre-Auger era is shown. An analysis of the longitudinal profile of the highest energy event reported by Fly's Eye showed incompatibility with photon primaries [16]. Studies of the data of inclined showers collected by Haverah Park excluded photons at 10^{19} eV at the 40% level [17]. This result is consistent with the analysis from the muon content of showers reported by AGASA [18]. The most stringent photon limit has recently been presented by the Auger Collaboration and it will be discussed in Section 5.3.

4 The Pierre Auger Observatory

The questions raised by the results concerning spectral shape, anisotropy, and composition of ultra-high-energy cosmic rays described above clearly indicate the need for greater statistics in the upper end of the CR spectrum, with accurate measurements of primary energies. The need for new experiments, with full sky coverage and uniform exposure for anisotropy studies, as well as new techniques to determine the composition in a Monte Carlo independent fashion was evident, and it was one of the reasons for the construction of Auger.

4.1 Hybrid detectors

The Pierre Auger Observatory has been developed by a team of over 400 scientists and technicians from 70 institutions in 17 countries. Auger is designed to measure the energy, arrival direction, and primary species with unprecedented statistical precision. The main feature of Auger is its unique capability of working in a hybrid detection mode. Particle showers are simultaneously observed by a ground array

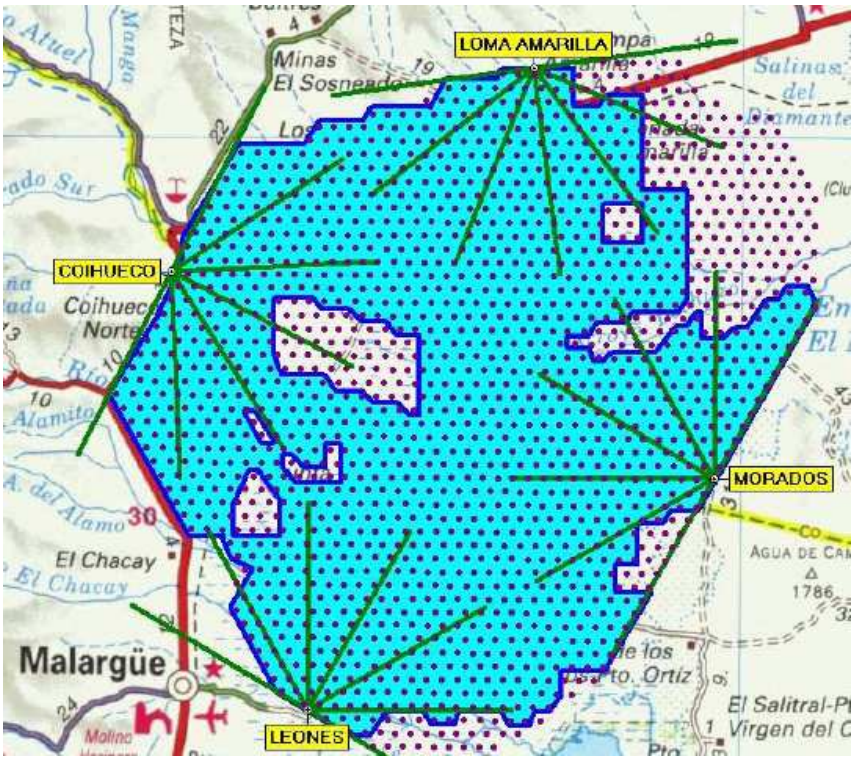

Fig. 4: The status of the Auger Observatory in early July 2007. At this time all 24 fluorescence detectors (located at the points marked Leones, Morados, Loma Amarilla and Coihueco) were operational and 1438 tanks had been deployed with 1364 taking data. The black dots mark the positions of the water-tanks.

and by fluorescence detectors. Ground detectors sample the particles of the extensive air shower hitting the ground, while fluorescence detectors follow the development of the shower in the atmosphere by detecting the fluorescence light produced by the interaction of charged secondaries [25].

The construction of the Southern Site of Auger began in 2000 at the foot of the Andes in the middle west of Argentina. When completed in late 2007 the Observatory will comprise 1600 particle detectors covering an area of 3000 km^2, overlooked by four fluorescence detectors. The surface array stations are water Čerenkov detectors (WCDs) spaced 1.5 km from each other in an hexagonal grid. Figure 4 shows the layout of the Argentinian site with the position of the surface array detectors and the fluorescence eyes at the periphery (Los Leones, Coihueco, Los Morados and Loma Amarilla). As at 9 July 2007, 1438 water-tanks had been deployed, with 1364 currently taking data.

The water Čerenkov detection technique and the fluorescence technique, both used in previous experiments, working together are the most powerful instrument for the observation of the extensive air shower properties and hence the study of UHECRs. Approximately 10% of the showers detected by Auger are observed by both surface and fluorescence detectors, allowing control of unwanted systematics in the primary energy determination. Thus, the hybrid data set is used to intercalibrate the detectors, providing confidence in the surface array results alone. The hybrid data set also provides a distribution function in multidimensional parameter space consisting of the quantities sensitive to the mass composition making it possible to constrain the choice of high-energy hadronic interaction models.

4.2 Ground array

The secondary particles produced by a cosmic-ray particle can be detected with stations deployed on a regular grid at the observing level. The ground array of the Pierre Auger Observatories consists of 1600 WCDs. Each detector is a cylindrical, opaque tank of 10 m^2 with a water depth of 1.2 m, where

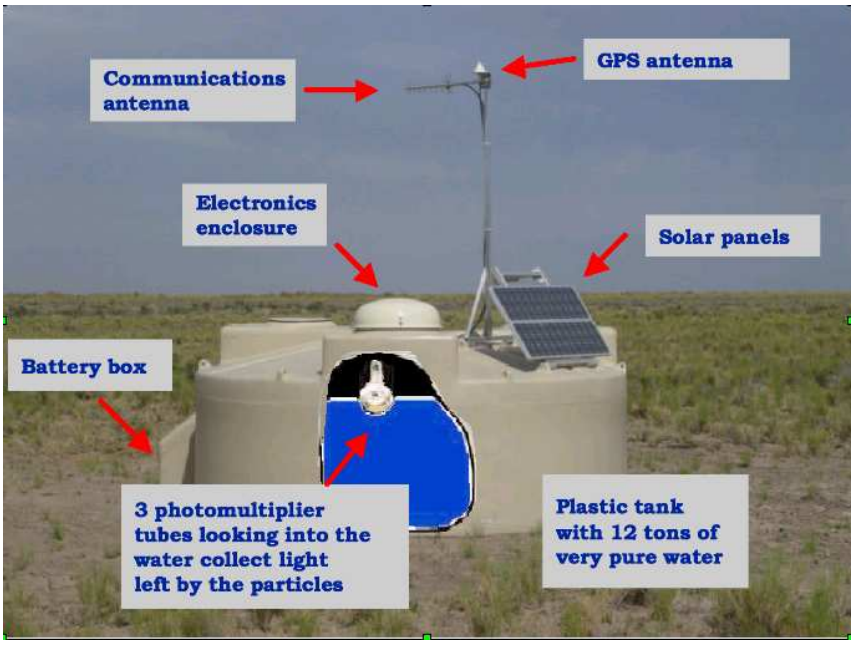

Fig. 5: A typical surface detector. See the text for a description of the components of the station.

particles produce light by Čerenkov radiation. The filtered water is contained in an internal coating which diffusely reflects the light collected by three photomultipliers (PMTs) installed on the top. The large-diameter PMTs ($\approx$ 20 cm) hemispherical photomultiplier are mounted face down and look at the water through sealed polyethylene windows that are an integral part of the internal liner. The signals are processed locally and a second-level trigger is identified before transmitting the data to the central acquisition system. Water tanks allow the detection of the very numerous photons present in showers. In addition, the depth enables showers to be detected efficiently over a wide angular range. Because of the size of the array the stations have to work in an autonomous way. Thus the stations operate on battery-backed solar power and communicate with a central station by using wireless LAN radio links. The time information is obtained from the Global Positioning Satellite (GPS) system. Figure 5 shows a water Čerenkov detector installed in the Southern Observatory. Mounted on top of the tank are the solar panel, electronic enclosure, mast, radio antenna, and GPS antenna for absolute and relative timing. A battery is contained in a box attached to the the tank.

4.3 Fluorescence detectors and the benefits of the hybrid mode

The Auger fluorescence detectors are expected to be operated always in conjunction with the surface detectors. The amount of fluorescence light emitted is proportional to the number of charged particles in the showers allowing a direct measurement of the longitudinal development of the EAS in the atmosphere. For this, the sky is viewed by many segmented eyes using photomultipliers. From the measured shower profile the position of the shower maximum $X_{\rm max}$ can be obtained. The energy in the electromagnetic component is calculated by integrating the measured shower profile. Corrections for atmospheric attenuation of the fluorescence light and contamination of the signal by Čerenkov light have to be made, using monitoring details at the observatory [26].

A good shower reconstruction by means of the fluorescence detectors ($X_{\rm max}$ resolution $\approx$ 20 g cm^{-2}) depends on the ability to determine the position of the shower axis inside the shower-detector plane (the plane in space containing the shower axis and a point representing the detector). This is done using the light arrival times in each pixel, see Fig. 6. However, a better determination of the shower axis is achieved if the shower is observed in the hybrid mode, using timing information from the SD [27]. The

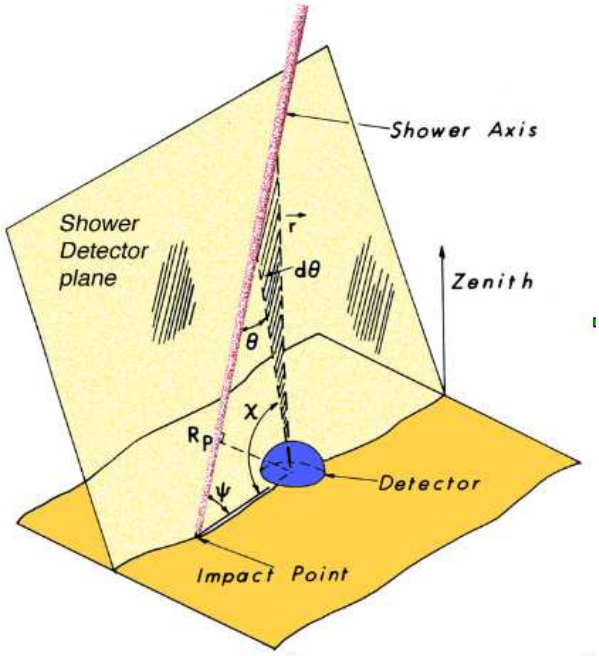

Fig. 6: Geometry of an EAS trajectory as seen by the fluorescence detector. The shower detector plane contains both EAS and the centre of the detector.

timing information acts as a powerful constraint to the geometrical reconstruction of the event such that the accuracy of the measurement of the distance of an FD to the shower axis and the angular accuracy in determining the direction are both improved by a factor of 10. Good determination of the shower axis is mandatory for good energy and mass composition assignments.

Four fluorescence detectors with 24 telescopes installed at the periphery of the ground array are working, and thus over 85% of the observatory is operational at present. For the design of the fluorescence telescopes the principle of a wide Schmidt camera is used. Figure 7 shows the main components of a fluorescence eye: a large spherical mirror with a radius of curvature of 3.4 m, a pixel camera with 440 PMTs in the focal surface, and a diaphragm with an entrance glass window. This filter allows reduction of night background with respect to the fluorescence signal and also serves to protect the equipment from dust. Each fluorescence detector is housed in a single building. A picture of the FD building at Los Leones taken from the 50-metre concentrator tower for data transmission is shown in Fig. 8.

5 Results from the Pierre Auger Observatory

5.1 Energy spectrum

The hybrid nature of the Auger Observatory enables the energy spectrum of primary particles to be determined without strong dependence on the mass and hadronic interaction models. The method used at the Pierre Auger Observatory is simple and it uses the strengths of both fluorescence and surface array techniques. This approach is to use a very high quality sample of hybrid events in which the energy, estimated accurately using the fluorescence detectors, is related to the ground parameter estimator S(1000), the signal of the WCD at 1000 m from the core in units of VEM. One VEM is the the signal produced by a single vertical relativistic muon passing through the centre of a WCD. The parameter S(1000) is obtained from a fit to the lateral distribution signals. The analysis presented here was done with 357 hybrid events collected up to 28 February 2007, satisfying strict criteria. The selected events for the estimation of the CR spectrum have zenith angle less than 60° and reconstructed energy above 3 EeV where the array is fully efficient and the acceptance is solely determined by the geometric aperture of

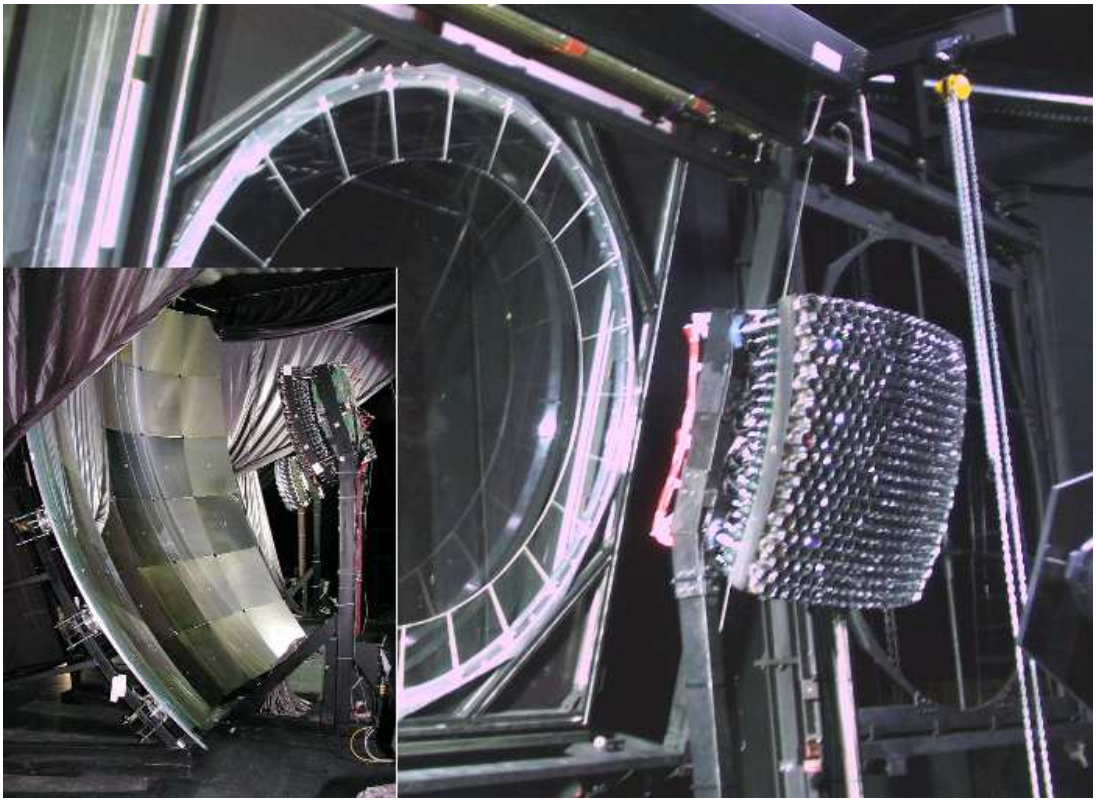

Fig. 7: Main components of a fluorescence telescope. See the text for a description of the components in the figure.

Fig. 8: A photo of the building for the fluorescence detectors at the Los Leones site (south of the surface array)

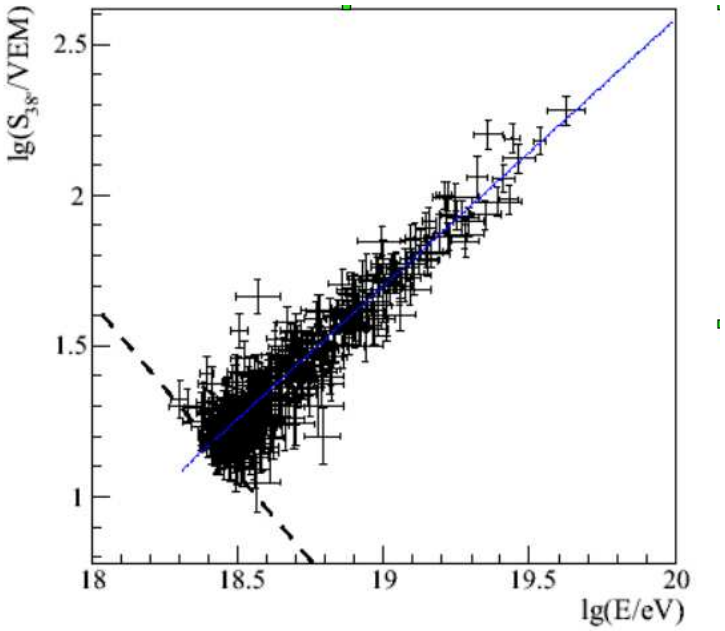

Fig. 9: The 387 events with simultaneous measurement of $S_{38}(1000)$ and an energy derived from the fluorescence detectors (taken from Ref. [29])

the array [28]. The integrated exposure up to 28 February 2007 is 5165 km^2 sr yr, about three times that achieved at AGASA and very similar to the monocular HiRes. Showers coming from different zenith angles give very different signals due to the flux attenuation in the atmosphere. So, before obtaining the relation between the energy estimator S(1000) and energy, the dependence of S(1000) on θ was empirically established using the Constant Intensity Cut (CIC) method. This method assumes that the cosmic rays arrive isotropically and hence the integral flux above a certain energy is independent of zenith angle. Details of the method are described in Ref. [29]. The calibration factor is obtained from the relation between S_{38}, the S(1000) parameter normalized to the mean zenith angle of events of 38° [1]. The calibration curve is shown in Fig. 9, the limited statistics leads to an uncertainty in the energy scale of 18%. In addition, there is a systematic uncertainty in the fluorescence measurement of 22%, which is dominated by the uncertainty in the fluorescence yield. The energy spectrum derived from nearly 12 000 SD events passing the selection criteria is discussed in Ref. [29].

Figure 10 shows the obtained energy spectrum multiplied by E^3 from SD data using showers above and below 60 ° [2], together with the spectrum derived from the hybrid sample [31]. An analysis of the implications of the spectrum derived by the Auger collaborations was presented in Ref. [32]. To analyse the upper part of the spectrum, a fit in the energy range [$10^{18.6}$ eV–$10^{19.6}$ eV] to a power-law function using a binned likehood method was performed. The slope of the spectrum is [–2.6± 0.03(stat) ± 0.02(sys)]. The expected number of events from such flux above $10^{19.6}$ eV and 10^{20} eV are 132 ± 9 and 30 ± 2.5, respectively, while the observed number of events are 58 and 2 events, respectively. Besides, the spectral index above $10^{19.6}$ is [–4.14 ± 0.42(stat)].

A close inspection of the spectrum in Fig. 10 indicates an ankle at around $10^{18.5}$ eV with a steepening about a decade higher. With the present statistics, the hypothesis that the cosmic-ray spectrum continues in the form of a power-law above $10^{19.6}$ eV is rejected with a 6 sigma significance, however, it is not clear that this result demonstrates the GZK prediction. A precise measurement of the energy, anisotropy, and primary mass is needed for a complete interpretation of the measured spectrum. Two

[1] The justification for the normalization to 38° is set out in Ref. [29].

[2] An additional exposure of 1510 km^2 sr yr is readily available by using events at large zenith angles. The method to estimate the energy for these events is described in Ref. [30].

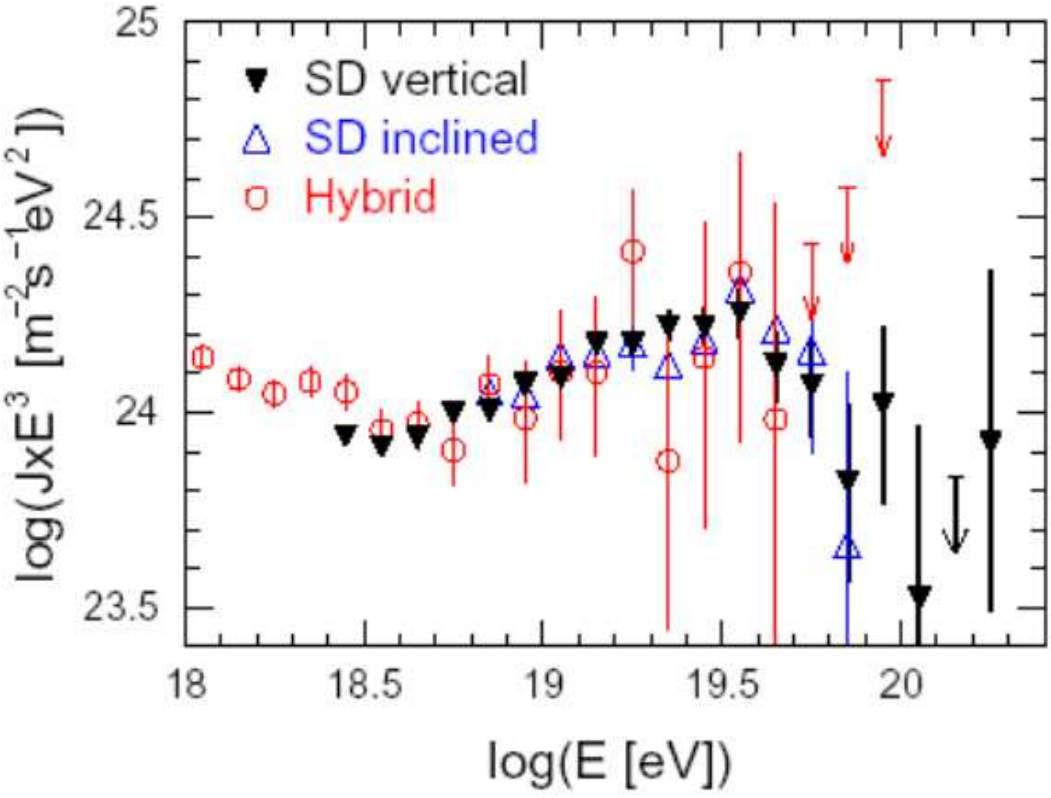

Fig. 10: Comparison of spectra measured with inclined events and with hybrid events

events with energies above 10^{20} eV have been detected, corresponding to a flux of ≈ 1 per km^2 per sr per millennium.

5.2 Arrival direction distributions

As mentioned above, a major aim of the Pierre Auger Collaboration is the identification of deviations from isotropy (the anisotropy) in the flux of cosmic rays. This aim is based on the expectation that rigidity-dependent propagation will begin to allow a form of directional astronomy with cosmic rays at the highest energies. In past studies, the inevitable statistical noise in the data, and subtle time variations in the array stability, have caused some claims to be made for observed anisotropies which have not been confirmed. This has partially resulted from an inadequate knowledge of the number of trials involved in the analysis. The Auger project aims to avoid the latter uncertainties by an *a priori* definition of the analysis process so that the chance probability of any positive detection can be rigorously evaluated.We will refer to this as an *a priori* analysis prescription. Exploratory searches beyond this prescription will be encouraged, but the Auger Collaboration will not assign any confidence level to anisotropies that may be discovered that way. Any such discovery would identify a good target for a prescription to be used with a subsequent Auger data set.

The Auger Collaboration have been searching for signals from the Galactic centre and for clustering at higher energies, as well as effects associated with BL Lacertae objects [33]. None of the earlier claims have been confirmed. Details of the searches made by the Auger Collaboration can be found in Refs. [34–37]. More statistics are needed to conclude about the arrival direction distribution of the highest energy cosmic rays.

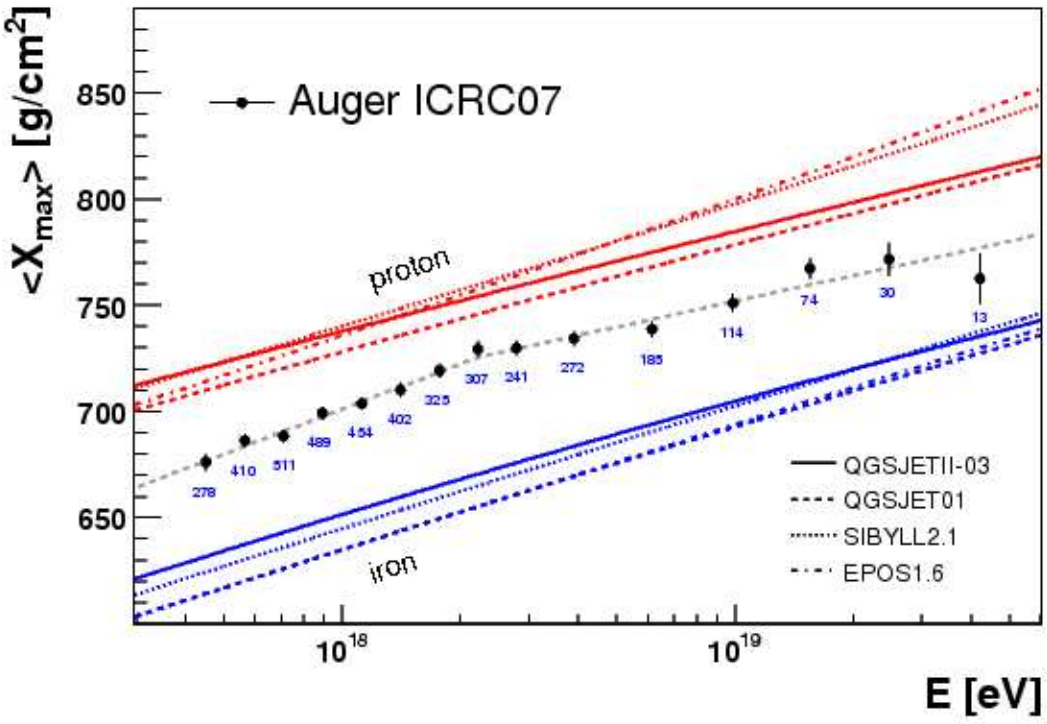

Fig. 11: The depth of shower maximum $X_{\max}$ as a function of energy. Taken from Ref. [38].

5.3 Mass composition

Baryonic species may, to some extent, be distinguished by the signatures they produce in the atmosphere. The main purpose of fluorescence detectors is to measure the properties of the longitudinal development. This is very important as the speed of shower development is the clearest indicator of the primary composition. For instance, nucleus-induced showers develop faster than proton showers, having $X_{\max}$ higher in the atmosphere. From Monte Carlo simulations, one finds that the difference between the average $X_{\max}$ for protons and iron nuclei is about 90–100 g cm^{-2}. However, because of shower-to-shower fluctuations, it is not possible to obtain meaningful composition estimates from $X_{\max}$ on a shower-by-shower basis, though one can derive composition information from the magnitude of the fluctuations themselves. For protons, the depth of first interaction fluctuates more than it does for iron, and consequently the fluctuations of $X_{\max}$ are larger for protons as well. These fluctuations depend only weakly on the choice of interaction model.

Using the data from the Pierre Auger Observatory, where the maxima can be found to an accuracy of ≈ 20 g cm^{-2} [38], a study of the cosmic-ray composition using events recorded in hybrid mode during the first years of data taking was performed. Each event used in such studies by the Auger Collaboration is a hybrid event in which at least one surface detector has been used to constrain the geometry of the reconstruction. The Auger results are shown in Fig. 11 where the average of measurements of $X_{\max}$ based on 4105 events across two decades of energy are shown together with predictions for proton and iron primaries made using three models of hadronic interactions. It is clear that a single slope does not fit the data and that the rate of increase of $X_{\max}$ with energy is smaller above 2×10^{18} eV than in the region below.

A preliminary conclusion from the data of Fig. 11 is that the mass spectrum is not proton dominated at the highest energies. This unexpected result assumes that the shower models are broadly correct. The position of each data point with respect to the model lines can be used to extract an estimate $\langle \ln A \rangle$, where A is the atomic mass.

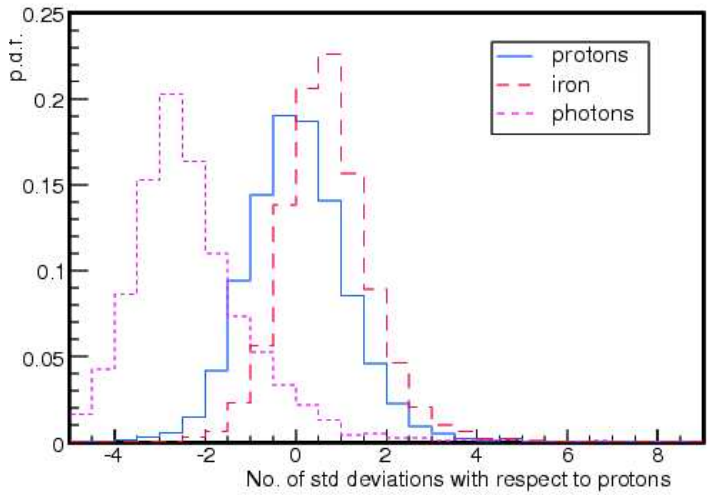

Fig. 12: Radii of curvature from simulations of proton, iron, and photon

In the following, a description of a mass composition analysis using data collected from the surface detectors of the Pierre Auger Observatory is presented [39]. The analyses are mainly based in the time structure of the shower front as measured with a 25 ns flash DC system of the WCD. The mass-sensitive parameters used are:

- the signal rise time at some distance from the shower core, the time to rise from 10% to 50% of the integrated signal;
- the curvature of the shower front;
- the muon content of the shower that can be assessed by looking for the tell-tale signs of sudden, large energy deposits in the time traces;
- the azimuthal asymmetry in the signal rise time within the shower plane.

In Fig. 12 a comparative radii of curvature from simulations of protons, iron and photons is shown. Muons, besides having larger energies at ground than electromagnetic particles, tend to arrive earlier and over a shorter period of time. Therefore, a shower with a larger number of muons will produce station triggers that are compact in time, resulting in a flatter shower front than for a similar shower that is muon-poor.

Evidence of azimuthal asymmetries in the time structure and signal size have been found in non-vertical showers at the Pierre Auger Observatory. It has been previously shown that the asymmetry in time distributions (such as rise time $\tau_{1/2}$) offers a new possibility for the determination of the mass composition [40]. If $\tau_{1/2}(r,\zeta) = a + b\cos\zeta$, the asymmetry factor b/a is sensitive to the distance between the detector and the shower maximum. New studies have demonstrated that the dependence of the asymmetry parameter in the rise time distributions with sec θ shows a clear peak. The position of the peak is different for proton and iron as shown in Fig. 13 reflecting the systematic difference in the average $X_{\rm max}$.

Auger data have also been used to set limits to the flux of photons above 10^{19} eV. Two methods have been adopted. The first [41] makes use of direct measurements of the depth of shower maximum made with the fluorescence detectors while the second uses the radius of curvature of the shower front and the time spread of the signals as measured with the surface detectors [42]. The observed distributions are compared with the predictions of Monte Carlo calculations for photon primaries. Showers produced by photons are expected to have larger values of $X_{\rm max}$, curvature, and time spread than showers produced by proton primaries. No photon candidates have been identified and a limit of 2% to the photon flux above 10^{19} eV has been set. The upper limits to the flux of photons along with predictions of top-down

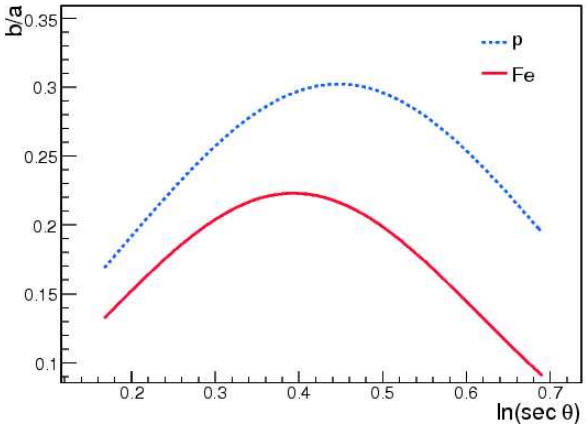

Fig. 13: Longitudinal development of the asymmetry factor in the rise time with zenith angle. Primary energy: $10^{18.5}$ eV.

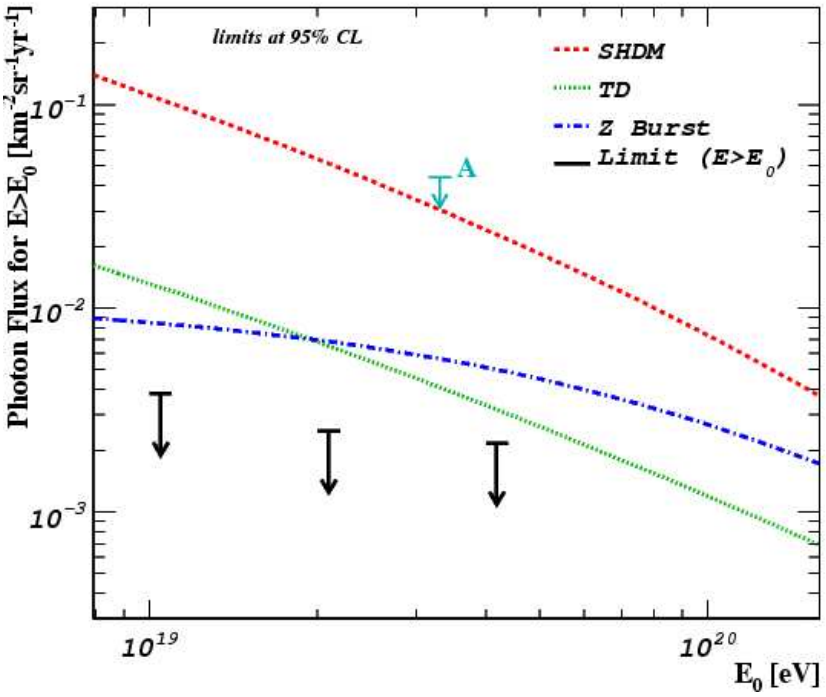

Fig. 14: Upper limits to the flux of photons

models are shown in Fig. 14. Label A in this figure refers to the limits set by AGASA. The significance of this result in the context of top-down models of ultra-high-energy cosmic rays is discussed in Ref. [42], and most models are ruled out.

Acknowledgements

I would like to thank the organizers for inviting me to present the Auger talk and for the warm hospitality. I am indebted to my Auger collaborators for many illuminating discussions.

References

[1] J. Linsley, *Phys. Rev. Lett.* **10** (1963) 146.

[2] D.J. Bird *et al.*, *Astrophys. J.* **441** (1995) 144.

[3] L. Anchordoqui, M.T. Dova, A. Mariazzi, T. McCauley, T. Paul, S. Reucroft and J. Swain, *Ann. Phys.* (NY) **314** (2004) 145, [arXiv:hep-ph/0407020].

[4] P. Blasi and E. Amato, arXiv:0706.1714 [astro-ph].

[5] P. Bhattacharjee and G. Sigl, *Phys. Rep.* **327** (2000) 109.

[6] A.V. Olinto, *Phys. Rep.* **329** (2000) 333.

[7] M. Hillas, *Annu. Rev. Astron. Astrophys.* **22** (1984) 425; P.L. Biermann, *J. Phys. G (Nucl. Part. Phys.)* **23** (1997) 1.

[8] R.D. Blanford, *Phys. Scripta* **T85** (2000) 191.

[9] J.P. Rachen and P.L. Biermann, *Astron. Astrophys.* **272** (1993) 161.

[10] K. Greisen, *Phys. Rev. Lett.* **16** (1966) 748; G.T. Zatsepin and V.A. Kuzmin, *JETP Lett.* **4** (1966) 78.

[11] C.T. Hill and D.N. Schramm, *Phys. Rev.* **D31** (1985) 5648;
V.S. Berezinsky and S.I. Grigoreva, *Astron. Astrophys.* **199** (1988) 1;
J.L. Puget, F.W. Stecker and J.H. Bredekamp, *Astrophys. J.* **205** (1976) 638;
S. Yoshida and M. Teshima, *Prog. Theor. Phys.* **89** (1993) 833;
L.A. Anchordoqui, M.T. Dova, L.N. Epele and J. Swain, *Phys. Rev.* **D55** (1997) 7356;
L.A. Anchordoqui, M.T. Dova, L.N. Epele and J. Swain, *Phys. Rev.* **D57** (1998) 7103;
L.N. Epele and E. Roulet, *JHEP* **9810** (1998) 009;
T. Stanev, R. Engel, A. Mucke, R. Protheroe and J.P. Rachen, *Phys. Rev.* **D62** (2000) 093005.

[12] M. Nagano *et al.*, *J. Phys.* **G18** (1992) 423.

[13] N. Hayashida *et al.*, *Astrophys. J.* **522** (1999) 225.

[14] C.C.H. Jui [HiRes Collaboration], *Proceedings of 27th International Cosmic Ray Conference*, Hamburg, **1** (2001) 354.

[15] M.T. Dova, A.G. Mariazzi and A.A. Watson, *Proceedings of 29th International Cosmic Ray Conference*, Pune, India (2005), e-Print: astro-ph/0512408.

[16] F. Halzen *et al.*, *Astropart. Phys.* **3** (1995) 151.

[17] M. Ave *et al.*, *Phys. Rev. Lett.* **85** (2000) 2244.

[18] K. Shinozaki *et al.* [AGASA Collaboration], *Proceedings of 27th ICRC*, Hamburg, **1** (2001) 346.

[19] B.R. Dawson, R. Meyhandan and K.M. Simpson, *Astropart. Phys.* **9** (1999) 331.

[20] M. Ave, L. Cazon, J.A. Hinton, J. Knapp, J. Lloyd-Evans and A.A. Watson, *Astropart. Phys.* **19** (2003) 61 [arXiv:astro-ph/0203150].

[21] M.T. Dova, M.E. Mancenido, A.G. Mariazzi, T.P. McCauley and A.A. Watson, *Astropart. Phys.* **21** (2004) 597–607 [astro-ph/0305351].

[22] M. Ave, J. Knapp, M. Marchesini, M. Roth and A.A. Watson, *Proceedings of 28th International Cosmic Ray Conference*, Tsukuba, **349** (2003).

[23] K. Shinozaki *et al.* [AGASA Collaboration], *Proceedings of 28th International Cosmic Ray Conference*, Tsukuba, **401** (2003);
K. Shinozaki, *Astrophys. J. Lett.*, **571** (2002) 117.

[24] G. Archbold *et al.*, *Proceedings of 28th International Cosmic Ray Conference*, Tsukuba, **405** (2003).

[25] J. Abraham *et al.* [Pierre Auger Collaboration], *Nucl. Instrum. Methods* **A523** (2004) 50.

[26] R. Cester [Pierre Auger Collaboration], *Proceedings of 27th ICRC*, Hamburg, (2001).

[27] B. Dawson and P. Sommers [Pierre Auger Collaboration], *Proceedings of 27th ICRC*, Hamburg (2001);
B. Dawson [Pierre Auger Collaboration], *Proceedings of 30th ICRC*, Merida, Mexico (2007).

[28] D. Allard [Pierre Auger Collaboration], *Proceedings of 29th ICRC*, Pune, India **7** (2005) 71.

[29] M. Roth [Pierre Auger Collaboration], *Proceedings of 30th ICRC*, Merida, Mexico (2007), arXiv:0706.2096 [astro-ph].

[30] P. Facal San Luis [Pierre Auger Collaboration], *Proceedings of 30th ICRC*, Merida, Mexico (2007), arXiv:0706.4322 [astro-ph].

[31] L. Perrone [Pierre Auger Collaboration], *Proceedings of 30th ICRC*, Merida, Mexico (2007), arXiv:0706.2643 [astro-ph].

[32] T. Yamamoto [Pierre Auger Collaboration], *Proceedings of 30th ICRC*, Merida, Mexico (2007), arXiv:0707.2638 [astro-ph].

[33] C.B. Finley and S. Westerhoff [HiRes Collaboration], *Proceedings of 29th ICRC*, Pune, India **7** (2005) 339; D.S. Gurbunov *et al.*, *JETP Lett.* **80** (2004) 145.

[34] E.M. Santos [Pierre Auger Collaboration], *Proceedings of 30th ICRC*, Merida, Mexico (2007), arXiv:0706.2669 [astro-ph].

[35] E. Armengaud [Pierre Auger Collaboration], *Proceedings of 30th ICRC*, Merida, Mexico (2007), arXiv:0706.2640 [astro-ph].

[36] S. Mollerach [Pierre Auger Collaboration], *Proceedings of 30th ICRC*, Merida, Mexico (2007), arXiv:0706.1749 [astro-ph].

[37] D. Harari [Pierre Auger Collaboration], *Proceedings of 30th ICRC*, Merida, Mexico (2007), arXiv:0706.1715 [astro-ph].

[38] M. Unger [Pierre Auger Collaboration], *Proceedings of 30th ICRC*, Merida, Mexico (2007), AIP Conf. Proc. **881** (2007) 220.

[39] M.D. Healy [Pierre Auger Collaboration], *Proceedings of 30th ICRC*, Merida, Mexico (2007), arXiv:0706.1569 [astro-ph].

[40] M.T. Dova, M. Mancenido, A.G. Mariazzi, F. Arqueros and D. Garcia-Pinto, *Proceedings of 29th ICRC*, Pune, India, arXiv:astro-ph/0507171.

[41] J. Abraham *et al.* [Pierre Auger Collaboration], *Astropart. Phys.* **27** (2007) 155 [arXiv:astro-ph/0606619].

[42] M.D. Healy [Pierre Auger Collaboration], *Proceedings of 30th ICRC*, Merida, Mexico (2007), arXiv:0710.0025 [astro-ph].